Published in final edited form as:
Int J Cancer. 2009 July 15; 125(2): 438–445. doi:10.1002/ijc.24345.

A new pulsed electric field therapy for melanoma disrupts the tumor's blood supply and causes complete remission without recurrence

Richard Nuccitelli[1,2,*], **Xinhua Chen**[1], **Andrei G. Pakhomov**[1], **Wallace H. Baldwin**[1], **Saleh Sheikh**[1,2], **Jennifer L. Pomicter**[1], **Wei Ren**[1], **Christopher Osgood**[1], **R. James Swanson**[1], **Juergen F. Kolb**[1], **Stephen J. Beebe**[1], and **Karl H. Schoenbach**[1,*]

[1] Frank Reidy Research Center for Bioelectrics, Old Dominion University, Norfolk, VA

[2] BioElectroMed Corp., Burlingame, CA

Abstract

We have discovered a new, ultrafast therapy for treating skin cancer that is extremely effective with a total electric field exposure time of only 180 μsec. The application of 300 high-voltage (40 kV/cm), ultrashort (300 nsec) electrical pulses to murine melanomas *in vivo* triggers both necrosis and apoptosis, resulting in complete tumor remission within an average of 47 days in the 17 animals treated. None of these melanomas recurred during a 4-month period after the initial melanoma had disappeared. These pulses generate small, long-lasting, rectifying nanopores in the plasma membrane of exposed cells, resulting in increased membrane permeability to small molecules and ions, as well as an increase in intracellular Ca^{2+}, DNA fragmentation, disruption of the tumor's blood supply and the initiation of apoptosis. Apoptosis was indicated by a 3-fold increase in *Bad* labeling and a 72% decrease in *Bcl-2* labeling. In addition, microvessel density within the treated tumors fell by 93%. This new therapy utilizing nanosecond pulsed electric fields has the advantages of highly localized targeting of tumor cells and a total exposure time of only 180 μsec. These pulses penetrate into the interior of every tumor cell and initiate DNA fragmentation and apoptosis while at the same time reducing blood flow to the tumor. This new physical tumor therapy is drug free, highly localized, uses low energy, has no significant side effects and results in very little scarring.

Keywords

nanosecond; pulsed electric fields; apoptosis; necrosis; angiogenesis

The most common treatment for skin cancer is the surgical removal of the lesion. This is time consuming and almost always leaves a scar. An alternative approach is electrochemotherapy in which the tumor is exposed to a toxic drug after electropermeabilization[1] using electric pulses in the microsecond domain. A third approach is irreversible electroporation that kills the treated tissue by necrosis resulting from permanent permeabilization using microsecond domain pulses with larger amplitudes.[2] We have discovered that if the electric pulses are shortened 1,000-fold into the nanosecond domain, they are able to independently initiate the process of apoptosis within the tumor cells themselves, causing the tumor to slowly self-destruct without requiring toxic drugs or permanent permeabilization.[3] In addition to initiating apoptosis in the tumor cells, nanosecond pulsed electric fields (nsPEFs) halt blood flow in the

*Correspondence to: Frank Reidy Research Center for Bioelectrics, Old Dominion University, 830 Southampton Avenue, Suite 5100, Norfolk, VA 23510, Fax: (757) 314-2397. E-mail: kschoenb@odu.edu or rich@bioelectromed.com.

capillaries feeding it. This reduced blood flow to the tumor and activation of apoptosis pathways cause the tumor to slowly shrink and disappear within an average of 47 days. This treatment exposure time is only 180 μsec, but we paused 2 sec between pulses to be sure that there would be no significant temperature increase. This resulted in a total treatment time of 10 min and resulted in little or no scarring.

The two main reasons that these nanosecond pulses are so effective is that (*i*) they are fast enough to penetrate into the cell and all organelles; and (*ii*) they are short enough that an electric field strength large enough to cause small pore formation in membranes can be used without significant heating. As long as the pulse rise time is faster than the characteristic cellular membrane charging time of about 0.1–1 μsec, the interior charges will not have sufficient time to redistribute to counteract the imposed field and it will penetrate into the cell and charge every organelle membrane for a duration, which is dependent on both the charging time constant of the cell's plasma membrane as well as that of the organelle membrane. Pulses 300 ns long are near the upper limit of this penetrating range and have the advantage of delivering an effective energy dose (0.2 J) without significantly heating the tumor.[4]

Material and methods

Pulsed electric field application

The generation of unipolar, high-voltage pulses with a duration between 100 and 600 nsec was based on the concept of transmission lines and pulse-forming lines as described in detail recently.[5] A matching resistor equal to the pulse generator impedance was placed in parallel with the load so that the total impedance would be to assure the delivery of a single well-defined trapezoidal pulse across the biological sample. We used 4 different configurations providing similar exposures in the experiments reported here: (*i*) all of the animal studies were conducted with a pulse-forming network with an impedance of 75 Ω. It consists of 30 pairs of high-voltage capacitors and 30 inductors arranged in a Blumlein configuration, and generates a 300-nsec long high-voltage pulse with a 30-ns rise time.[4,5] The closing switch consisted of a mercury displacement relay that was controlled by a microcontroller. The voltage across the object was monitored using a high-voltage probe (P6015A, Tektronix, Beaverton, CA), and the current was measured by means of a Pearson coil (model 2877, Pearson Electronics, Palo Alto, CA). Current and voltage were recorded simultaneously using a digitizing oscilloscope (TDS3052, Tektronix, Beaverton, OR). The electric field pulses were applied by lifting the skin containing each tumor away from the mouse between 2 fingers and gently placing the tumor between 2 polished parallel circular stainless steel electrodes on the end of a clothespin-shaped applicator. The electrodes were 5 mm in diameter and completely covered each tumor with a 1-mm space between the electrodes. The tumors sometimes slipped away from, this region while being squeezed between the plates, so pulses were usually applied in 3 groups of 100, at a frequency of 0.5 Hz and the electrodes were repositioned between each group of pulses to ensure that the entire tumor was being exposed to the field. (*ii*) For the intracellular Ca^{2+} studies, we used a 100 Ω Blumlein line coaxial cable pulse generator with a MOSFET closing switch (DE275-102N06A, IXYS, Milpitas, CA). The switch was triggered by a MOSFET driver (DEIC420, IXYS) which was, in turn, controlled by a 12-bit microprocessor (Analog Devices ADuC 841 Microconverter®). This pulse generator exhibited a rise time of 7 nsec and pulse duration of 100 nsec. (*iii*) For the comet studies, cells were placed in a cuvette with aluminum electrodes on 2 opposing inner walls and we used a 10 Ω transmission line pulse generator with a gap distance-adjusted self-breakdown spark gap as a closing switch, This pulse generator exhibited a rise time of 5 nsec and pulse duration of 300 nsec. (*iv*) For the patch-clamp experiments we used a 50 Ω transmission line circuit with a MOSFET closing switch (DE275-102N06A). The pulse generator delivers a 600-nsec pulse with a rise time of 4 nsec to a pair of tungsten wire electrodes. The wire diameter was 0.1 mm and the gap between them

was 0.11 and 0.12 mm. For convenience, the pulse generator was triggered by external TTL pulses using pClamp software and the Digidata board.

Cell culture

Mammalian cell lines used in this study were obtained from American Type Culture Collection (Manassas, VA). Murine melanoma (B16-F10) cells were grown in Dulbecco's Modified Eagle's Medium (ATCC Catalog No. 30-2002) supplemented with 10% fetal bovine serum (Atlanta Biologicals S11550, Norcross, GA), 2% L-glutamine, 100 IU/ml penicillin, 100 μg/ml streptomycin and 0.25 μg/ml amphotericin B (Cellgro/Mediatech 25-005-CI and 30-001-CI) in a 75 cm^2 culture flask maintained at 37°C with 5% CO_2 in air by a water-jacketed cell culture incubator. Cells used were between passages 7 and 19, and never allowed to reach greater than 75% confluency. Patch-clamp experiments used a murine pituitary cell line, GH3, cultured in Ham's F12K medium supplemented with 2.5% fetal bovine serum and 15% horse serum (Atlanta Biologicals).

Animals

Female SKH-1 hairless mice were injected beneath the skin at 1 location on the back with 10^6 B16-F10 cells using a protocol approved by the Eastern Virginia Medical School IACUC. If these tumors became ulcerated, the mouse was euthanized. In the nsPEF-treated group, 13 mice were 3 months old when injected with melanoma cells and 4 mice were 2 months old. In the control group, 4 were 4 months old, 10 were 3 months old and 4 were 2 months old when injected with melanoma cells

Patch-clamp setup and data acquisition

Pipettes for patch-clamp recording were manufactured from borosilicate glass (1B150F-4, World Precision Instruments, Sarasota, FL, or BF150-86-10, Sutter Instrument, Novato, CA). They were pulled to a tip resistance of 1.5–3 MΩ using a Flaming/Brown P-97 Micropipette puller (Sutter).

Exposures of individual cells to nsPEF and subsequent measurements of membrane resistance (R_m) were performed in a glass-bottomed chamber (Warner Instruments, Hamden, CT) mounted to the stage of an inverted microscope. The microscope was an Olympus IX71 (Olympus America, Center Valley, PA). A coverslip with cells was placed into the chamber filled with a bath buffer at room temperature, and an individual cell suitable for nsPEF exposure and patch-clamp recording was selected. The nsPEF-delivering electrodes and a glass micropipette were positioned next to the selected cell using MP-285 and MP-225 robotic micromanipulators (Sutter Instrument, Novato, CA).

Electrophysiology data were acquired using a Multiclamp 700B amplifier, Digidata 1322A or 1440A A-D converter, and pCLAMP10 software (MDS, Foster City, CA).

Intracellular Ca^{2+} measurement

B16 cells were loaded with 5 μM Fluo-4 AM in Hank's Buffered Salt Solution supplemented with 6.7 mM HEPES buffer and 2.5 mM glucose for 45 min in the dark at room temperature. Loading was performed at room temperature to minimize dye compartmentalization.[6,7] Extracellular Ca^{2+} was chelated by the addition of 5 mM EGTA to the buffer before applying nsPEFs. A glass coverslip electrode chamber was constructed for applying the nsPEF to the cells. The chamber was fabricated by first metalizing a No. 1 coverslip glass by thermal evaporation of chromium and nickel, then patterning a 30-μm thick positive photoresist electroplating mold, and finally electrodeposition from a nickel sulfamate plating bath with a gold top coat to ensure biological compatibility. This process yields electrodes that are

deposited directly onto the glass substrate with no intermediate glue layer. The electrode gap distance is 100 μm, allowing the application of electric fields of up to 100 kV/cm with a Blumlein line pulse generator charged to 1 kV. Five microliters of cells in phosphate-buffered saline (PBS) were placed into the electrode gap and covered with an 8-mm round coverslip. Experiments were performed at 37°C using a custom-made microscope objective heater. Confocal imaging was performed with a Perkin Elmer UltraVIEW spinning disk confocal imager mounted on an Olympus IX71 inverted microscope with a 60× oil immersion objective (numerical aperture of 1.42). To prevent evaporation, the round coverslip was sealed with pure silicone fluid (Clearco Products, Bensalem, PA) dispensed from a large plastic syringe with a luer stub anchored with epoxy. The electric pulses (40 kV/cm 100 nsec) were delivered by a MOSFET-triggered Blumlein coaxial cable pulse generator attached to 25-μm thick electrodes initially vacuum deposited and then electroplated onto a glass coverslip while maintaining a 100-μm gap between the 2 parallel electrodes (BioElectroMed Corp., Burlingame, CA).

Immunocytochemistry

Tumors were fixed in 10% buffered formalin overnight and processed for histology. Serial tissue sections were deparaffinized and antigen retrieval was achieved by microwaving for 10 min in 0.01 M citrate buffer (pH 6.0). The following antibodies were used to label the slides: Bcl-2(C-2), Bad(H-168) (Santa Cruz Biotechnology, Santa Cruz, CA) Microvessel density was identified by incubating sections for 1 hr with anti-mouse CD31 antibody (M-20; Santa Cruz Biotechnology). Tissue microarrays were adopted for homogeneity and high-throughput analysis. One section was stained with hematoxylin–eosin (H&E) for histopathological diagnosis before immunocytochemistry. The percentage of each section stained with 1 of these antibodies was determined by using Photoshop's Magic Wand to cut out the labeled region of each slide and Image J was then used to determine the percentage of each section covered by the label.

DNA fragmentation assay

B16-F10 mouse melanoma cells, passage numbers 5–15, were collected and washed in PBS. One hundred forty microliters of cells (1×10^5 cells/ml) were placed in disposable cuvettes with parallel plate, aluminum electrodes on 2 sides (Biosmith Biotech, 1 mm gap) and pulsed using parameters similar to those used for *in vivo* experiments described above (typically, 300 nsec pulse duration, 40 kV/cm, pulse numbers 10–100). Control cells were pipetted into cuvettes, and held under identical conditions to those cells subjected to nsPEFs. After pulsing, 10-μl aliquots of cells were withdrawn and mixed with 100 μl of 2% low-melting agarose in PBS (Amresco, Agarose II) at 30°C. Seventy-five microliters of the cell mixture was spread onto glass slides and allowed to gel at room temperature. The slides were then processed essentially as described in Refs. 8 and [9]. Slides were immersed in chilled lysis buffer (1.24 mM NaCl, 200 mM EDTA, 10 mM Tris–HCl, 34 mM sarkosyl, 10 mM Triton-X 100, pH 10.0) for 1 hr. The slides were then placed in a horizontal electrophoresis chamber, submerged in alkaline electrophoresis buffer (300 mM NaOH, 1 mM EDTA, pH > 13) and held at room temperature for 30 min. They were then exposed to 2.5 V/cm for 30 min at room temperature. The slides were rinsed twice in excess neutralization buffer (0.4 M Tris–HCl, pH 7.5), briefly rinsed with water, and then stained with propidium iodide (210 μg/ml). Cells were imaged with an Olympus DP70 digital camera using fluorescent microscopy with a mercury lamp and TRITC filter set (exciter filter: 510–550 nm; 570nm dichroic; barrier: 590 longpass). Images were analyzed for comet quantification using CometScore software (TriTek Corp).

Results

We generated 1 melanoma in each of 35 SKH-1 albino, hairless, immune-competent mice by injecting 10^6 murine B16-F10 cells just under the skin on the back of each animal. Within 3

days, these cells formed a melanoma with a discoid shape 3–4 mm in diameter and about 1-mm thick that exhibited angiogenesis. These melanomas can be best observed in albino mice because their skin is translucent. When the skin containing the tumor is stretched over a light source, the pigmented tumor and blood supply are very clear. Digital images of the tumor using this transillumination technique with a stereoscope provide a very accurate assessment of tumor size and blood supply (Fig. 1*a*; day 0). Eighteen of these tumors served as controls and were not treated (Fig. 1*a*). Their continued growth caused 39% to become ulcerated within 16–21 days, at which time those mice were euthanized. The survival curve for the controls (Fig. 1*d*) indicates when each had to be euthanized and only 3/18 were still alive 6 months after melanoma cell injection. The melanomas had stopped growing in these 3 controls but residual melanin was still present.

We treated 17 of the melanomas with 1–3 applications of either 300 or 600 electric pulses (40–50 kV/cm, 70–90 A, 300 nsec, 0.5 Hz). We demonstrated previously that this treatment of only 90–180 μsec of total field exposure time does not heat the tumor more than 3°C but is sufficient to cause the tumor to shrink by 90% within 2 weeks.[4] Our goal here was to determine if these melanomas could be completely eliminated, without recurrence, using only 1–3 nsPEF treatments.

Twenty-four percent of the melanomas exhibited complete remission with a single nsPEF treatment

Mouse 219's melanoma was 1 of the 4 melanomas that responded to a single nsPEF treatment with complete remission (Fig. 1*a*). For each indicated day after treatment, both the transillumination and the reflected light images are shown. Note that the capillaries feeding the tumor begin to breakdown after treatment (0*) and are completely gone by day 6. By day 29, the tumor was also essentially gone and did not recur over the 144 days that we followed it before euthanizing the animal. We observed a similar time course for the other 3 animals whose tumors disappeared after a single nsPEF treatment.

Fifty-nine percent of the melanomas exhibited complete remission with 2 nsPEF treatments

We photographed each tumor every 2 to 3 days to determine if it was beginning to grow again. Once we detected regrowth, we treated the tumor with 300 more pulses using the same parameters as described above. Mouse 180's melanoma (Fig. 1*b*) is typical of 10 of the 17 tumors that responded to 2 nsPEF treatments with complete remission. Comparing the melanoma size on days 11 and 13 suggested possible regrowth, which was even clearer on day 14, so we treated the tumor again on that day. Two weeks later, the tumor was barely visible and no recurrence could be detected by day 169 when we euthanized the animal. A small residual pigment spot could be detected in some of the animals, but it did not change over months of observation, and histological analysis confirmed that no tumor cells were present.

Eighteen percent of the melanomas required 3 nsPEF treatments for complete remission

Three of the 17 melanomas began growing again after 2 treatments so a third nsPEF treatment was administered to those (M205, Fig. 1*c*). All of these melanomas exhibited complete remission after the third nsPEF treatment and did not recur.

Figure 1 illustrates the changes in melanoma size during the nsPEF treatment times. We also present a more complete photographic record for 3 other nsPEF-treated melanomas in Figure 2. All of the nsPEF-treated melanomas shrink in surface area by 90% on average within 2 weeks.

How do these pulses trigger the self-destruction of melanoma tumors?

We have identified several cellular targets affected by these ultrashort electric pulses including tumor blood flow, membrane conductance, intracellular Ca^{2+}, DNA fragmentation, microvessel disruption and the initiation of apoptosis.

nsPEF application rapidly reduces blood flow to the tumor

Transillumination images clearly show that the blood vessels feeding these tumors before pulsing disappear within a day after pulsing (Figs. 1 and 2). This disruption of blood flow to the tumor stresses these rapidly dividing cells and many exhibit necrosis. The remainder of the tumor cells exhibit apoptosis as shown below. There is also a reduction in microvessels in the tumor as discussed below (Figs. 7*e* and 7*f*).

nsPEF application changes membrane conductance

We used whole cell patch clamp to measure plasma membrane conductance changes in a murine pituitary cell line, GH3, resulting from nanosecond pulsed electric field exposure and have detected unique “nanopores” generated in the plasma membrane after nsPEF exposure. We call them nanopores because membrane-impermeant dyes, such as trypan blue or propidium iodide, do not pass through them in contrast to the pores generated by classical electroporation (Figs. 3*b* and 3*c*). Surprisingly, this increase is not due to the formation of a nonspecific pore in the membrane. If these nanopores were simply holes, their I–V characteristic would be a straight line, linear at any voltage and crossing the abscissa at or near 0 mV. The actual conductance is very different. There is a good deal of inward current at negative potentials, but no positive (outward) current at positive potentials (Fig. 4*d*). So, the nanopores exhibit inward rectification along with inhibition of voltage-gated outward K^+ current at positive membrane potentials. These behaviors clearly distinguish the permeability increase resulting from nsPEF application from that resulting from the application of much longer pulses used for classical electroporation. Two other important characteristics of the nsPEF-induced permeability increase are that it is long lasting, and it increases with field strength. Whole cell membrane conductance measured 2–3 min after exposure to a single pulse of 2.4 or 4.8 kV/cm exceeded the control values 4–5-fold and about 10-fold, respectively. These lower pulse amplitudes were chosen because they generated nanopores without electronic disturbance to the patch-clamp computer.

nsPEF application triggers increases in intracellular Ca^{2+}

We imaged the intracellular Ca^{2+} changes in cultured B16-F10 cells loaded with Fluo-4AM in response to nsPEF on a spinning disk confocal microscope (PerkinElmer Ultraview, Waltham, Massachusetts). Intracellular Ca^{2+} increased immediately after nsPEF application because of both release from intracellular stores and Ca^{2+} influx through the plasma membrane. By chelating extracellular Ca^{2+} with 5 mM EGTA, we determined that 45% of the total Ca^{2+} change is due to release from intracellular stores (Fig. 5). Cells recovered from this increased Ca^{2+} within 90 sec at 37°C (inset, Fig. 5). We averaged the fluorescence signal from 10 to 20 cells taken from multiple fields of view and on different days to obtain the data illustrated in Figure 5. Because our melanoma tumor treatment exposed the tumor cells to 1 pulse every 2 sec, intracellular Ca^{2+} would have been elevated for 10 min during a 300-pulse exposure.

nsPEF application triggers DNA fragmentation

Because pyknosis of tumor cell nuclei was evident in histological sections of fixed tumors as soon as 10 min after nsPEF exposure,[4] we used the comet assay to examine DNA fragmentation. We found that fragmentation occurs very rapidly after nsPEF application and the degree of fragmentation increases with pulse number (Fig. 6). We have observed this fragmentation in response to nsPEF of different pulse widths (60, 100 and 300 nsec) and

observed some DNA repair if we delayed permeabilization of the cells for the comet assay for an hour (data not shown). We find that the degree of DNA fragmentation *in vitro* is linearly proportional to the square root of the pulse number Figure 6*b*. This may be related to our observation that 1 and 10 pulses have little effect on the tumors but 100 pulses strongly triggers apoptosis.[4]

nsPEF application triggers apoptosis in vivo

Bcl-2 is a family of proteins involved in the response to apoptosis. Some of these proteins (such as *Bcl-2* and *Bcl-XL*) are antiapoptotic, whereas others (such as *Bad*, *Bax* or *Bid*) are proapoptotic. The sensitivity of cells to apoptotic stimuli can depend on the balance of pro- and antiapoptotic *Bcl-2* proteins. We investigated the involvement of *Bcl-2* and *Bad* using immunohistochemistry on sections from both nsPEF-treated and untreated tumors. We observed an average decrease of 74% in the antiapoptotic *Bcl-2* labeling when comparing 9 nsPEF-treated tumors to 9 untreated tumors (Fig. 7). In contrast, the apoptotic label, *Bad*, increased by an average of 320% ($n = 8$ treated and 8 untreated). Both of these changes suggest that nsPEF initiates apoptosis in the tumor cells *in vivo.*

nsPEF application changes microvessel density

Tumor growth depends on a local increase in vasculature, which requires the formation of new capillaries in a process known as angiogenesis. Endothelial cells forming capillaries can be detected with antibodies to the endothelial cell marker, CD31.[10] We reported previously that nsPEF disrupts blood flow to larger melanomas based on power Doppler data from high-resolution ultrasound, but that technique cannot detect microvessels.[4] Here, we used immunocytochemistry to detect endothelial cell density in both nsPEF-treated and untreated sections from 5 different melanomas and found an average reduction of 92% in CD31 expression in nsPEF-treated tumors (Figs. 7*e* and 7*f*). This suggests that the microcirculation to the treated tumors is severely reduced and this should lead to necrosis and tumor shrinkage.

Discussion

The use of nsPEF to eliminate skin tumors is a new approach that has several major advantages over conventional therapies. It is very fast, 100% effective, and causes minimal skin scarring by initiating apoptosis pathways in which the tumor slowly self-destructs. Two other therapies that have used electric fields are electrochemotherapy and irreversible electroporation. The former allows the introduction of toxic drugs to the tumor by electroporation and the latter uses much longer pulses (100 μsec) of 2.5 kV/cm amplitude to permeabilize cells irreversibly to cause necrosis.[2,11] Both of these approaches are fundamentally different from the use of nsPEF. Although nsPEF does cause some necrosis by sharply reducing the blood supply to the tumor, much of the self-destruction involves apoptosis resulting in tumor resorption over an average of 47 days. This much slower elimination of the tumor results in less scar formation and no recurrence of the tumor, which is a major advantage over irreversible electroporation, which kills by necrosis alone.

Another therapy that uses electric fields, typically in the radio frequency band, is hyperthermia. This approach kills the tumor by heating it to temperatures greater than 42°C for several minutes. Because tissues conduct heat quite well, it is impossible to exclusively heat the tumor without heat transfer to tissues that are in contact with it. One distinct advantage of nsPEF over hyperthermia is the ability to more sharply localize target tissues because only cells located between the electrodes are exposed to the nsPEF. An additional advantage is the much shorter treatment time for nsPEF. Although we used a 10-min treatment time (0.5 Hz) to be certain that we would not heat the tumor more than 3°C as documented in our previous article,[4] the tumor temperature increase levels off after the initial 2 min of pulse application. Therefore, it

is likely that higher pulse application frequencies could be used without significant temperature increases and that could substantially shorten the total treatment time.

How does nsPEF treatment lead to apoptosis and DNA fragmentation? Several previous studies of cells *in vitro* have provided very strong evidence that nsPEF application triggers apoptosis[12,13] and increases in intracellular Ca^{2+}[14–18] in Jurkat, HL-60 and chromaffin cells. These previous studies were all conducted at room temperature, whereas those reported here were conducted at 37°C. At room temperature, we would predict that the recovery from the Ca^{2+} increase would be slower because of the slower kinetics of the Ca^{2+} pumps. That seems to be the case for HL-60 and Jurkat cells, but chromaffin cells actually recover faster.[17] Another interesting characteristic of chromaffin cells is that most of the Ca^{2+} enters from the outside rather than from the internal stores.

NsPEF application to melanomas *in vivo* also triggers apoptosis and (Fig. 7) but in addition has other effects, such as the reduction in blood flow to the tumor and the increase in intracellular Ca^{2+}. Both of these latter changes are important signals for initiating tumor cell death. If intracellular Ca^{2+} remains high for several minutes, it can initiate several metabolic cascades that will lead to cell death and DNA fragmentation.[19,20] The formation of nanopores leads to an increase in intracellular Ca^{2+}, and both the electric field strength and pulse number influence this permeability increase. The larger the pulse number and the electric field, the larger will be the permeability increase in the plasma membrane[21–23] that will lead to a long-lasting increase in intracellular Ca^{2+}.

This nsPEF therapy has also been used to treat skin tumors by another group at the University of Southern California.[24] They have found it effective against pancreatic tumors developing from cells injected beneath mouse skin as well as for a single case of a human basal cell carcinoma that exhibited complete remission after 1 treatment with nsPEF with very little scarring (200 pulses, 20 nsec long, 43 kV/cm). This suggests that this new therapy, which has proven very effective for treating mouse skin cancer, might be equally as effective on humans.

Acknowledgments

This work was supported by grants from the Air Force Office of Scientific Research, BioElectroMed Corp., a gift from Mr. Frank Reidy and internal funds of the Frank Reidy Research Center for Bioelectrics at Old Dominion University.

Grant sponsors: Air Force Office of Scientific Research, BioElectroMed Corp., Frank Reidy Research Center for Bioelectrics at Old Dominion University.

References

1. Kubota Y, Tomita Y, Tsukigi M, Kurachi H, Motoyama T, Mir LM. A case of perineal malignant melanoma successfully treated with electrochemotherapy. Melanoma Res 2005;15:133–4. [PubMed: 15846147]
2. Al-Sakere B, Andre F, Bernat C, Connault E, Opolon P, Davalos RV, Rubinsky B, Mir LM. Tumor ablation with irreversible electroporation. PLoS ONE 2007;2:e1135. [PubMed: 17989772]
3. Schoenbach KH, Hargrave B, Joshi RP, Kolb JF, Nuccitelli R, Osgood C, Pakhomov AG, Stacey M, Swanson RJ, White JA, Xiao S, Xiao S, et al. Bioelectric effects of intense nanosecond pulses. IEEE Trans Dielectr Electr Insul 2007;14:1088–109.
4. Nuccitelli R, Pliquett U, Chen X, Ford W, James SR, Beebe SJ, Kolb JF, Schoenbach KH. Nanosecond pulsed electric fields cause melanomas to self-destruct. Biochem Biophys Res Commun 2006;343:351–60. [PubMed: 16545779]
5. Kolb JF, Kono S, Schoenbach KH. Nanosecond pulsed electric field generators for the study of subcellular effects. Bioelectromagnetics 2006;27:172–87. [PubMed: 16304697]

6. Nuccitelli, R. A practical guide to the study of calcium in living cells. San Diego: Academic Press; 1994.
7. Simpson, A. Fluorescent measurement of $[Ca^{2+}]_c$ basic practical considerations. In: Lambert, DG., editor. Methods in molecular biology. Vol. 114. Totowa: Humana Press; 2005.
8. Singh NP, McCoy MT, Tice RR, Schneider EL. A simple technique for quantitation of low levels of DNA damage in individual cells. Exp Cell Res 1988;175:184–91. [PubMed: 3345800]
9. Collins AR. The comet assay for DNA damage and repair: principles, applications, and limitations. Mol Biotechnol 2004;26:249–61. [PubMed: 15004294]
10. Folpe AL, Cooper K. Best practices in diagnostic immunohistochemistry: pleomorphic cutaneous spindle cell tumors. Arch Pathol Lab Med 2007;131:1517–24. [PubMed: 17922587]
11. Rubinsky B. Irreversible electroporation in medicine. Technol Cancer Res Treat 2007;6:255–60. [PubMed: 17668932]
12. Beebe SJ, Fox P, Rec LJ, Somers K, Stark RH, Schoenbach KH. Nanosecond pulsed electric field (nsPEF) effects on cells and tissues: apoptosis induction and tumor growth inhibition. IEEE Trans Plasma Sci 2002;30:286–92.
13. Beebe SJ, Fox PM, Rec LJ, Willis EL, Schoenbach KH. Nanosecond, high-intensity pulsed electric fields induce apoptosis in human cells. FASEB J 2003;17:1493–5. [PubMed: 12824299]
14. Vernier PT, Sun Y, Marcu L, Salemi S, Craft CM, Gundersen MA. Calcium bursts induced by nanosecond electric pulses. Biochem Biophys Res Commun 2003;310:286–95. [PubMed: 14521908]
15. White JA, Blackmore PF, Schoenbach KH, Beebe SJ. Stimulation of capacitative calcium entry in HL-60 cells by nanosecond pulsed electric fields. J Biol Chem 2004;279:22964–72. [PubMed: 15026420]
16. Vernier PT, Sun Y, Wang J, Thu MM, Garon E, Valderrabano M, Marcu L, Koeffler HP, Gundersen MA. Nanoelectropulse intracellular perturbation and electropermeabilization technology: phospholipid translocation, calcium bursts, chromatin rearrangement, cardiomyocyte activation, and tumor cell sensitivity. Conf Proc IEEE Eng Med Biol Soc 2005;6:5850–3. [PubMed: 17281590]
17. Vernier PT, Sun Y, Chen MT, Gundersen MA, Craviso GL. Nanosecond electric pulse-induced calcium entry into chromaffin cells. Bioelectrochemistry 2008;73:1–4. [PubMed: 18407807]
18. Scarlett SS, White J, Blackmore PF, Schoenbach KH, Kolb J. Regulation of intracellular calcium concentrations by nanosecond pulsed electric fields. Biochim Biophys Acta. 10.1016/j.bbamem. 2009. 02.006
19. Szondy Z. Adenosine stimulates DNA fragmentation in human thymocytes by Ca^{2+}-mediated mechanisms. Biochem J 1994;304:877–85. [PubMed: 7818494]
20. Dong Z, Saikumar P, Weinberg JM, Venkatachalam MA. Calcium in cell injury and death. Annu Rev Pathol 2006;1:405–34. [PubMed: 18039121]
21. Pakhomov AG, Kolb JF, White JA, Joshi RP, Xiao S, Schoenbach KH. Long-lasting plasma membrane permeabilization in mammalian cells by nanosecond pulsed electric field (nsPEF). Bioelectromagnetics 2007;28:655–63. [PubMed: 17654532]
22. Pakhomov AG, Shevin R, White JA, Kolb JF, Pakhomova ON, Joshi RP, Schoenbach KH. Membrane permeabilization and cell damage by ultrashort electric field shocks. Arch Biochem Biophys 2007;465:109–18. [PubMed: 17555703]
23. Frey W, White JA, Price RO, Blackmore PF, Joshi RP, Nuccitelli R, Beebe SJ, Schoenbach KH, Kolb JF. Plasma membrane voltage changes during nanosecond pulsed electric field exposure. Biophys J 2006;90:3608–15. [PubMed: 16513782]
24. Garon EB, Sawcer D, Vernier PT, Tang T, Sun Y, Marcu L, Gundersen MA, Koeffler HP. *In vitro* and *in vivo* evaluation and a case report of intense nanosecond pulsed electric field as a local therapy for human malignancies. Int J Cancer 2007;121:675–82. [PubMed: 17417774]

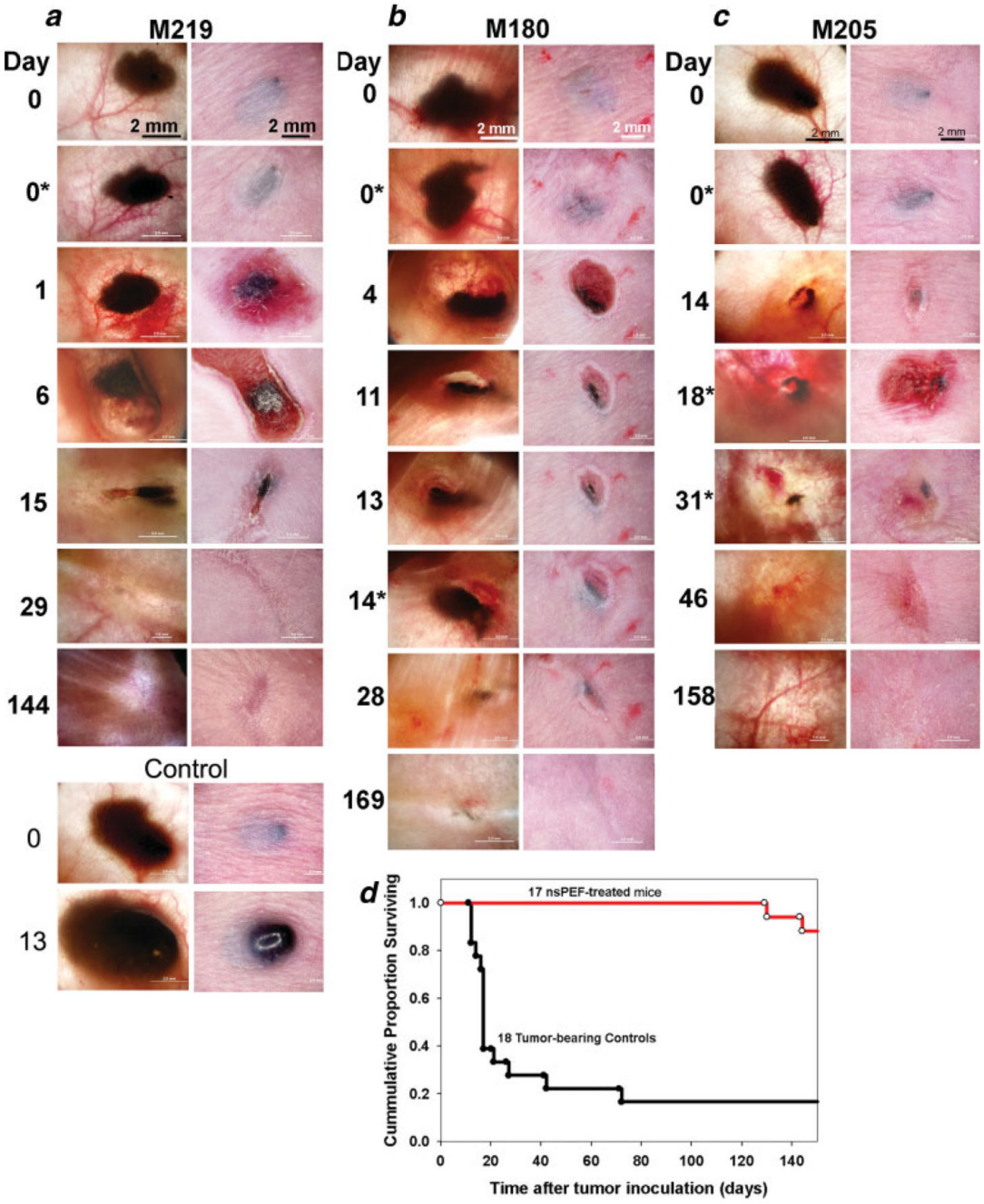

Figure 1.

Tumor responses to nsPEF. (*a*) Transillumination and surface views of a melanoma in mouse 219 that responded with complete remission after a single treatment of 300 pulses (40 kV/cm, 300 nsec) on day 0. The asterisk indicates the day on which nsPEF was applied and the adjacent photos were taken shortly after nsPEF treatment. The cultured melanoma cells were injected beneath the skin 3 days before this image was taken and angiogenesis is already evident. The capillaries near the tumor begin to breakdown after nsPEF treatment. For comparison, 1 of the untreated control tumors is shown below. The 2-mm bar in the top images applies to all frames below them, (*b*) Mouse 180 is typical of 10 melanomas that exhibited total remission of the tumor after 2 nsPEF treatments. Melanoma shrinkage is documented by transillumination and

reflected light photomicroscopy after treatments of 600 pulses (40 kV/cm, 300 ns) on day 0 and 300 pulses on day 14. The tumor did not recur through day 169 when mouse 180 was euthanized. Each pair of images was taken on the day after nsPEF treatment indicated by the numbers on the left. The image pairs on day 0 were taken before (0) and after (0*) 300 pulses of 40 kV/cm, 300 nsec. The tumor did not recur through day 169 when mouse 180 was euthanized. (*c*) Mouse 205 is typical of 3 mice that exhibited total remission of the tumor after 3 nsPEF treatments. Melanoma shrinkage is documented by transillumination and reflected light photomicroscopy after treatments of 300 pulses (40 kV/cm, 300 nsec) on days 0, 18 and 31. Each pair of images was taken on the day indicated by the far left column. No recurrence of the tumor occurred through day 158 when mouse 205 was euthanized. The asterisk indicates the days on which nsPEF was applied. (*d*) Survival curve for 17 nsPEF-treated mice and 18 untreated controls with 1 melanoma each. All 17 treated mice exhibited complete tumor remission without recurrence during 150 days before euthanizing. One of these mice was euthanized on day 130 because of a 20% weight loss in a week but did not exhibit metastasis to the lungs or liver. A second treated mouse was euthanized on day 144 because of an eye infection. Controls were euthanized when tumors ulcerated.

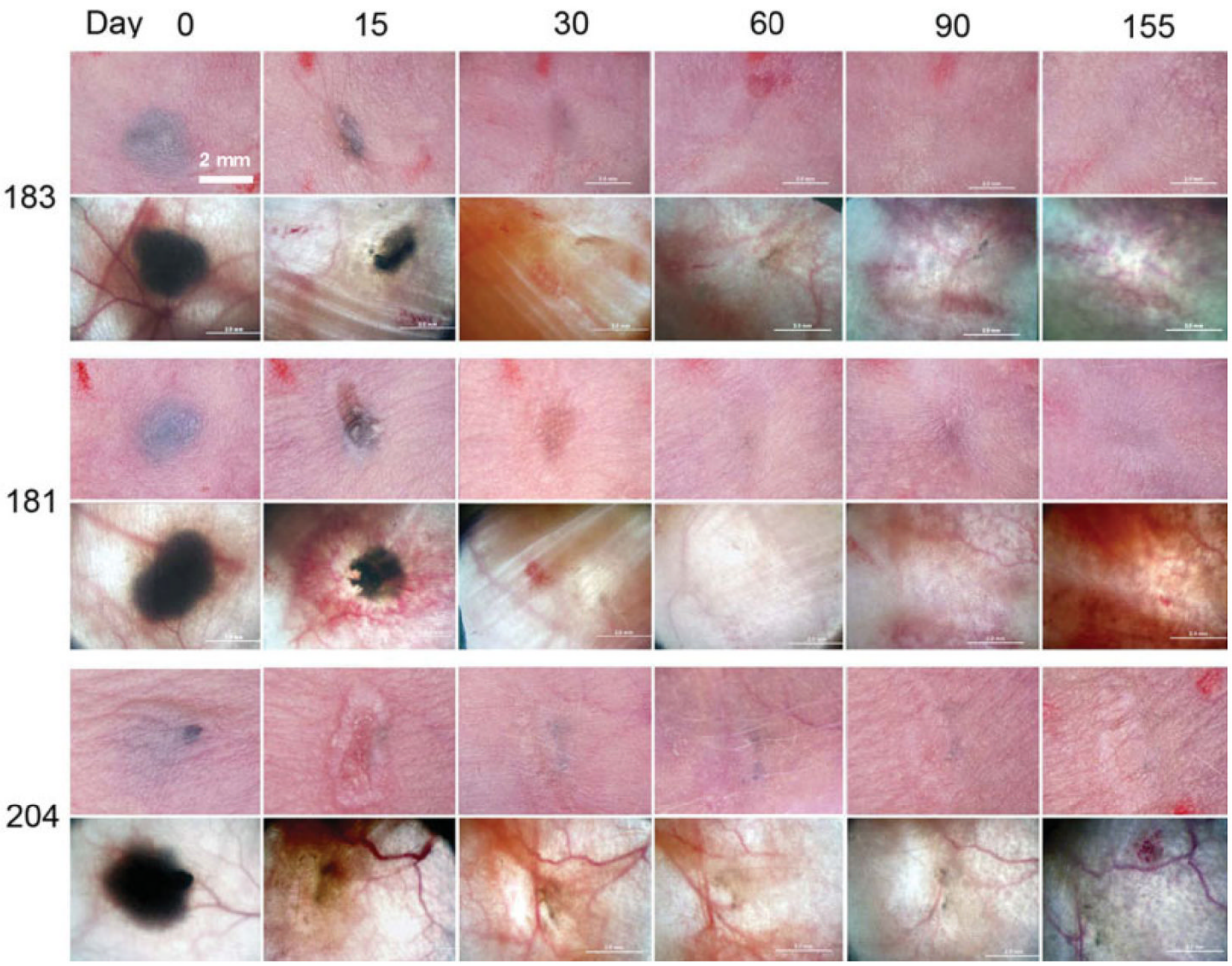

Figure 2.

Photomicrographs of 3 melanomas taken on the day indicated for each column after nsPEF treatment. Rows are grouped in matched pairs with the top image of the pair being the surface view and the bottom image being the transillumination view of the tumor. All images were taken at the same magnification indicated by the scale bar in the upper left image. The animal number is shown to the left of each grouped pair. Mouse 183 and 181 were treated on day 0 with 600 pulses (45 kV/cm, 300 nsec long) and again on day 18 with 300 pulses. Mouse 204 was only treated once on day 0 with 300 pulses (40 kV/cm, 90 A, 300 nsec) and the tumor exhibited total remission following this single treatment. The scale bar in the upper left photo applies to all of these images. Red tattoo marks were used to indicate the original tumor location.

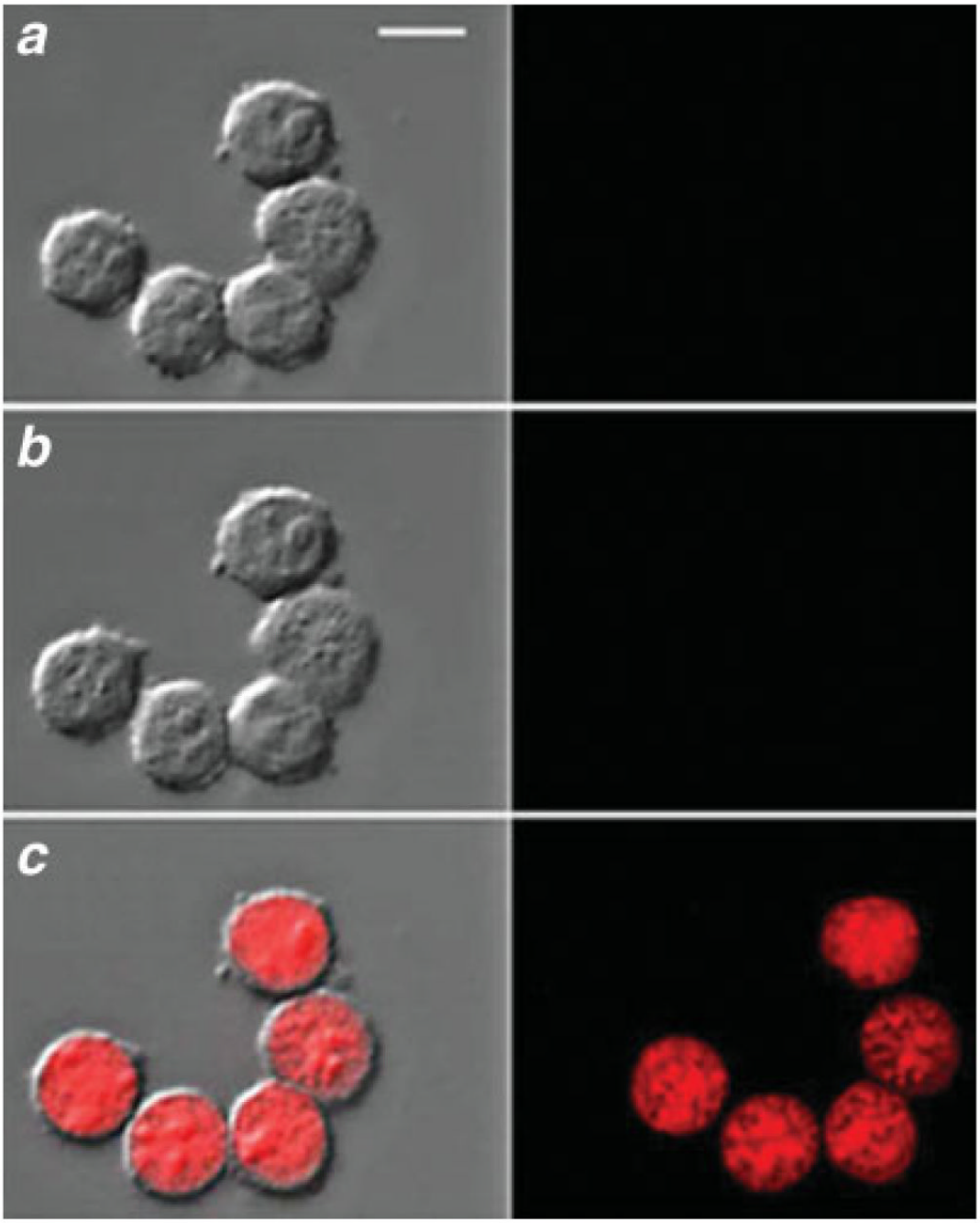

Figure 3.

Lack of propidium iodide (PI) uptake after nsPEF exposure, GH3 cells were exposed to 2 Hz train of ten 600-nsec pulses at 4.2 kV/cm in the medium containing 20 μg/ml PI (other components, mM: 135 NaCl, 5 KCl, 2 $MgCl_2$, 10 HEPES and 10 glucose). The images were captured immediately before (*a*) and 300 sec after the exposure (*b*). Right panel: PI fluorescence channel. Left panel: PI fluorescence overlaid with a DIC image. Exposure caused minor morphological changes (swelling, blebbing, granulation), but no PI uptake. (*c*) Positive control: same cells 20 sec after membrane permeabilization by addition of digitonin (0.1%), Calibration bar: 10 μm. Note that this nsPEF exposure was far more intense than required for a profound

effect on the electrical conductance of plasma membrane (*e.g.*, Fig. 3*d*). This result was consistently observed in more than 6 experiments.

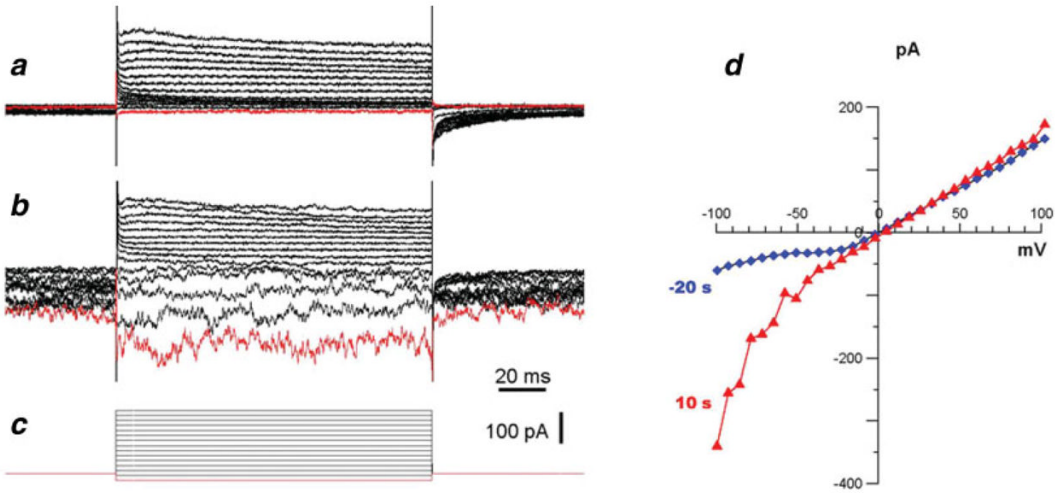

Figure 4.

Changes in the electrical conductance of the plasma membrane resulting from a 600-nsec electric pulse. (*a*) Whole-cell currents in a GH3 cell elicited by voltage steps from −100 to +100 mV (shown in *c*) 20 sec before nsPEF exposure. Patch pipette was filled with the extracellular solution containing (mM) 140 Cs-acetate, 5 Cs-EGTA, 4 $MgCl_2$ and 10 HEPES. (*b*) Recording from the same cell 10 sec after a single 600 nsec pulse at 2.4 kV/cm. The orientation of the applied nsPEF was perpendicular to the axis of the patch electrode so that the electrode would not interfere with the electric field's effect on the cell. (*d*). Current–voltage curves corresponding to A and B. Note profound increase of the mean inward current and "noise" at negative transmembrane voltages and lack of changes at positive voltages. Exposed cells could recover completely, but the process typically took several minutes (data not shown).

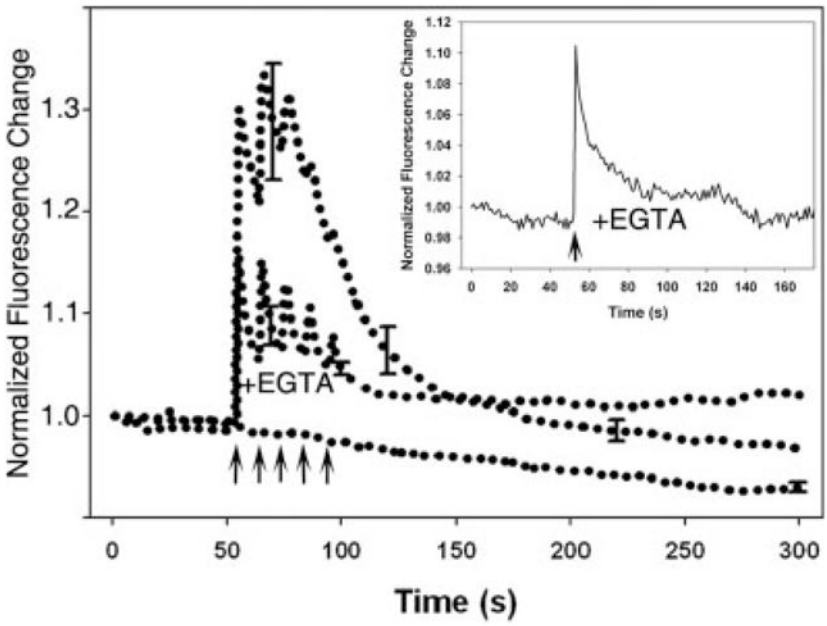

Figure 5.

Average intracellular Ca^{2+} changes in 10–20 B16-F10 cells loaded with Fluo-4AM when pulsed at the times marked by the arrows (40 kV/cm, 100 nsec) at 37°C. Top curve represents the average Ca^{2+} increase in normal medium, middle curve represents the average intracellular Ca^{2+} increase in Ca^{2+}-free medium (5 mM EGTA) and the lowest curve represents the average cellular fluorescence when no pulses were applied. Instead of plotting all of the SEMs, only the largest S.E.M. in each region of the curve is plotted. Inset figure shows the Ca^{2+} change in 1 cell triggered by a single 100-nsec pulse of 40 kV/cm in Ca^{2+}-free medium.

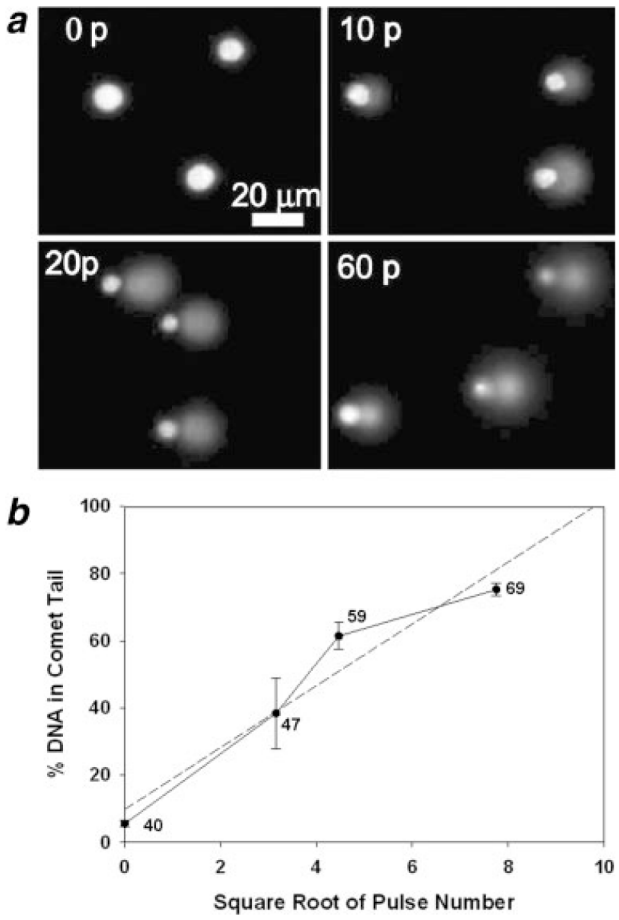

Figure 6.

DNA fragmentation is evident after nsPEF application using the Comet assay with B16 cells *in vitro*, *(a)* After the application of 40 kV/cm pulses 300 nsec long using the number of pulses indicated in the upper left corner of each frame, DNA fragmentation occurs as indicated by the comet tails in the figure. (*b*) Quantification of propidium iodide fluorescence allows us to estimate the percentage of total DNA in the comet tail. When plotted against the square root of pulse number, a linear dependence is revealed that predicts 100% DNA fragmentation when cells are exposed to 100 pulses. The straight line is a least squares fit to the 4 data points and the error bars represent the S.E.M. with the number of cells averaged for each point printed next to it.

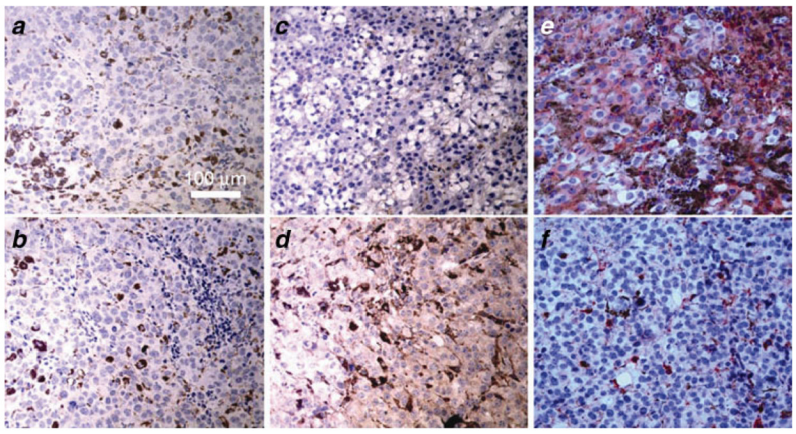

Figure 7.

Immunocytochemistry of control and nsPEF-treated tumors (300 pulses, 40 kV/cm) using antibodies to *Bcl-2*, *Bad* and CD31. (*a*) Control tumor labeled with antibodies to *Bcl-2;* (*b*) nsPEF-treated tumor labeled antibodies to *Bcl-2* 1 week after nsPEF treatment; (*c*) control tumor labeled with antibodies to *Bad;* (*d*) nsPEF-treated tumor labeled with antibodies to *Bad.* 1 week after nsPEF treatment; (*e*) control tumor labeled with anti-endothelial cell antigen (CD31); and (*f*) nsPEF-treated tumor labeled with antibodies to CD31one week after nsPEF treatment.